NOTATION

a = heat exchanger cost parameter
A_{C_K} = exchange area for steam heater on stream C_K (m^2)
A_{H_L} = exchange area for water cooler on stream H_L (m^2)
A_J = exchange area for exchanger J (m^2)
b = heat exchanger cost parameter
C = symbol indicating stream requires cooling water
C_K = cold stream K ($K = 1, 2, 3, \ldots, M$)
H = symbol indicating stream requires steam heating
H_L = hot stream L ($L = 1, 2, 3, \ldots, N$)
I = random integer between the values I_A and I_B
I_A = lower bound of positive integer variable x_i
I_B = upper bound of positive integer variable x_i
J = integer assigned to each exchanger in the array ($J = 1, 2, 3, \ldots, MN$)
k = distribution coefficient (positive odd integer)
k_d = range reduction coefficient (positive integer)
M = total number of streams to be heated
N = total number of streams to be cooled
N_t = number of independent variables
Q_J = heat transfer in exchanger J (Joules/s)
R = random positive real number
R_i = search region for variable x_i about x_i^*
T = symbol indicating stream requires no utilities to meet process temperature requirements
U = utilities cost per year for the network ($/yr)
x_i = new value of independent variable ($i = 1, N_t$)
x_i^* = value of variable x_i producing the best value for the objective function
Y = cost per year for the entire system ($/yr)
δ = annual rate of return on the investment
θ = random number between zero and one

LITERATURE CITED

Campbell, J. R., and J. L. Gaddy, "Methodology for Simultaneous Optimization with Reliability: Nuclear PWR Example," *AIChE J.*, **22**, No. 6, 1050 (1976).

Gall, D. A., "A Practical Multifactor Optimization Criterion," in *Recent Advances in Optimization Techniques*, A. Lavi and T. P. Vogl, ed., Wiley, New York (1966).

Hendry, J. E., and R. R. Hughes, "Generating Separation Process Flowsheets," *Chem. Eng. Progr.*, **68**, 71 (1972).

Heuckroth, M. W., L. D. Gaines, and J. L. Gaddy, "An Examination of the Adaptive Random Search Technique," *AIChE J.*, **22**, No. 4, 744 (1976).

Keenan, J. H., and F. G. Keyes, *Thermodynamic Properties of Steam*, Wiley, New York (1936).

Kesler, M. G., and R. O. Parker, "Optimal Networks of Heat Exchange," *Chem. Eng. Progr. Symposium Ser. No. 92*, **65**, 111 (1969).

King, C. J., D. W. Gantz, and F. J. Barnes, "Systematic Evolutionary Process Synthesis," *Ind. Eng. Chem. Process Design Develop.*, **11**, 271 (1972).

Kobayashi, S., T. Umeda, and A. Ichikawa, "Synthesis of Optimal Heat Exchange Systems," *Chem. Eng. Sci.*, **26**, 1367 (1971).

Lee, K. F., A. H. Masso, and D. F. Rudd, "Branch and Bound Synthesis of Integrated Process Designs," *Ind. Eng. Chem. Fundamentals*, **9**, 48 (1970).

Luus, R., and T. H. I. Jaakola, "Optimization by Direct Search and Systematic Reduction of the Size of Search Region," *AIChE J.*, **19**, 760 (1973).

Masso, A. H., and D. F. Rudd, "The Synthesis of System Designs," *ibid.*, **15**, 10 (1969).

Menzies, M. A., and A. L. Johnson, "Synthesis of Optimal Energy Recovery Networks Using Discrete Methods," *Can. J. Chem. Eng.*, **50**, 290 (1972).

Pho, T. K., and L. Lapidus, "Synthesis of Optimal Heat Exchanger Networks by Tree Searching Algorithms," *AIChE J.*, **19**, 1182 (1973).

Rathore, R. N. S., and G. J. Powers, "A Forward Branching Scheme for the Synthesis of Energy Recovery Systems," *Ind. Eng. Chem. Process Design Develop.*, **14**, 175 (1975).

Rathore, R. N. S., K. A. Van Wormer, and G. J. Powers, "Synthesis Strategies for Multicomponent Separation Systems with Energy Integration," *AIChE J.*, **20**, 491 (1974).

Rudd, D. F., G. J. Powers, and J. J. Siirola, *Process Synthesis*, Prentice-Hall, Englewood Cliffs, N.J. (1973).

Siirola, J. J., "Status of Heat Exchanger Network Synthesis," paper presented at 76th National AIChE Meeting, Tulsa, Okla. (Mar., 1974).

Manuscript received January 14, 1977; revision received July 19, and accepted August 11, 1977.

Effects of Temperature on the Crystallization of Potassium Nitrate by Direct Measurement of Supersaturation

JAMES E. HELT

and

MAURICE A. LARSON

Department of Chemical and Nuclear Engineering and Engineering Research Institute
Iowa State University
Ames, Iowa

A laboratory continuous mixed-suspension, mixed-product- removal crystallizer was used to study the effects of temperature on the kinetics of crystallization of potassium nitrate. A differential refractometer was used to continuously monitor the supersaturation permitting the measurement of supersaturation levels of order 10^{-3}Kg solute/Kg water. The nucleation rate exhibited an inverse relationship with temperature.

SCOPE

Attainment of the desired size distribution is one of the principal objectives in the design and operation of industrial crystallizers. The main factor which determines size distribution is the crystallization kinetics. If improvements are to be made in crystallizer design and operation, knowledge about the crystallization kinetics is needed.

Correspondence concerning this paper should be addressed to James E. Helt, North Carolina State University, Raleigh, North Carolina.

The overall kinetics is composed of two separate mechanisms, crystal growth and crystal nucleation. In many crystallizers, growth and nucleation are occurring simultaneously, which means they are competing for the available solute.

Since both nucleation and growth are direct functions of the level of supersaturation in the crystallizer, it is important to know what level of supersaturation exists. Normally, the magnitude of supersaturation is quite small in a mixed-suspension, mixed-product-removal (MSMPR) cooling crystallizer, making the measurement of supersaturation concentration very difficult. In most research to date, the relative magnitude of supersaturation has been inferred from the resulting crystal size distribution rather than the more desirable situation of predicting the crystal size distribution from knowledge of the level of supersaturation.

The objectives of this work are twofold: first, to use differential refractive index methods to measure the level of supersaturation in an MSMPR crystallizer and second, to develop the needed relationships relating the birth and growth rates of crystals to the level of supersaturation and to the crystallizer temperature.

CONCLUSIONS AND SIGNIFICANCE

1. It has been demonstrated that differential refractometer methods can be used effectively to measure levels of supersaturation of order 10^{-3} g solute/g of water. Although there was some scatter of the data, clear relationships were determined between the crystallization kinetic rates of potassium nitrate and supersaturation and temperature. Moreover, these kinetic relationships can be determined under conditions where both nucleation and growth are occurring to a measurable extent.

2. Further evidence obtained was that the supersaturation range where secondary nucleation does not occur coincides with the higher-order portion of the growth-supersaturation curve and, therefore, corresponds to the region of supersaturation where very low growth occurs. This supports the conclusion that secondary nucleation is closely related to growth.

3. Finally, this work confirms previous qualitative evidence that secondary nucleation is an inverse function of temperature for potassium nitrate. This observation can be explained by, and adds additional support to, the secondary nucleation theory which assumes a fluidized layer of unincorporated solute at the surface of a growing crystal being dislodged by crystal-apparatus contact.

A knowledge of the kinetics of a crystallization system is the key to understanding the factors influencing crystal size distribution (CSD). This is evident in the results of the work of Randolph and Larson (1971) in their studies of a mixed-suspension, mixed-product-removal (MSMPR) crystallizer. At steady state and when McCabe's ΔL law holds, such a crystallizer produces a crystal size distribution given by

$$n = n^o \exp(-L/G\tau) \tag{1}$$

The nuclei population density n^o is related to the nucleation rate B^o by

$$B^o = n^o G \tag{2}$$

Thus, the nucleation rate and the growth rate enter directly into the mathematical description of the size distribution.

Nielsen (1964) notes that power law functions of supersaturation approximate theoretical expressions, and Randolph and Larson (1971) and others (Genck, 1969; Kern and Abegg, 1973; Shor and Larson, 1971) have used power law expressions of the form

$$B^o = K_1(c - c_s)^m = K_1 s^m \tag{3}$$

Growth rate can also be related to supersaturation using power law kinetics:

$$G = K_2 s^n \tag{4}$$

It is frequently difficult to accurately know the supersaturation in a crystallizing system because of the very low level which normally exists. Consequently, investigators have combined Equations (2), (3), and (4) to obtain

$$n^o = K_N G^{i-1} \tag{5}$$

Equation (5) has been used to determine the order of nucleation m without the necessity of measuring supersaturation. Moreover, Equation (5), if known, provides a relationship between the competing kinetics of nucleation and growth and sets the limitation on the attainable size distribution.

Most crystallization systems exhibit secondary nucleation effects. When secondary nucleation is present, it is necessary to use a kinetic model which accounts for the nuclei formation directly related to the solids in suspension. K_1, used in Equation (3), must then be defined as

$$K_1 = K_1' M_T^j \tag{6}$$

In this case, K_1' accounts for the temperature effects as well as other effects in the system, and M_T^j accounts for the secondary nucleation effects. Equation (3) then becomes

$$B^o = K_1' M_T^j s^m \tag{7}$$

Using this model, Equation (5) becomes

$$n^o = K_1' M_T^j G^{i-1} \tag{8}$$

where the temperature dependency of both nucleation and growth is included in K_N'. In order to determine the effect of temperature on the individual kinetic rates, it is necessary to independently measure supersaturation so that the rate constants in Equations (3) and (4) can be determined.

In this work, the very low supersaturations exhibited by potassium nitrate were measured in order to determine the temperature dependence of nucleation rate.

Solution concentration may be determined directly by analysis or indirectly by measuring some property of the system that is a sensitive function of concentration. The direct methods are either gravimetric determination or

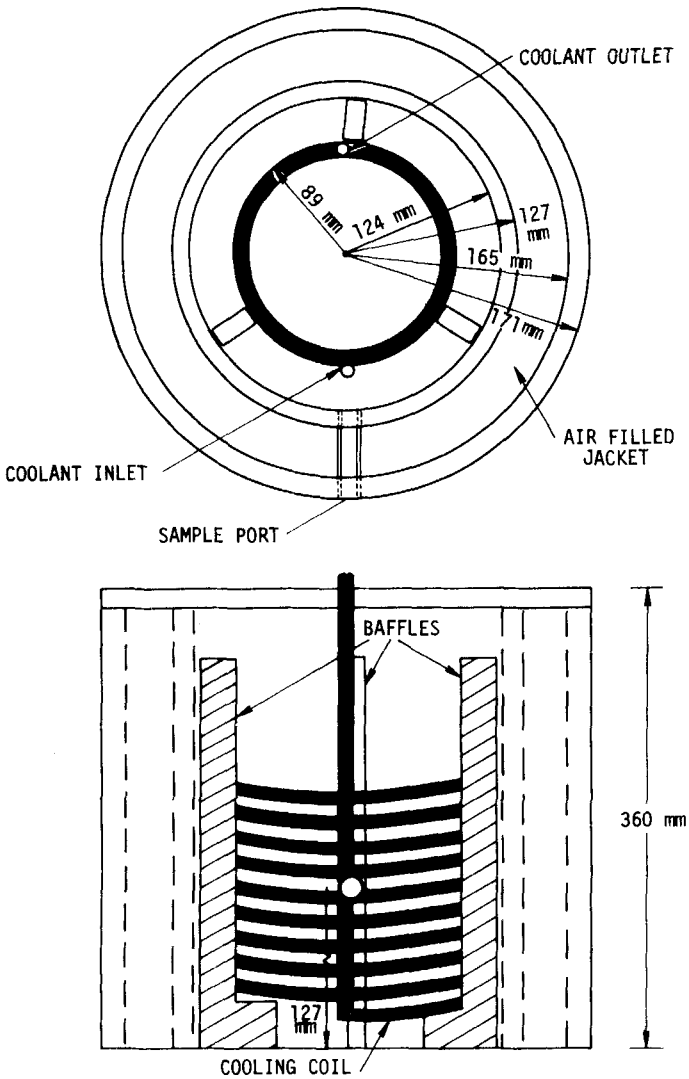

Fig. 1. Crystallizer vessel.

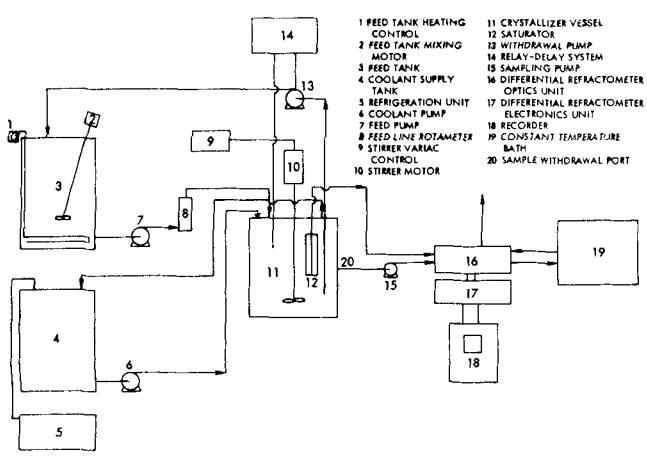

Fig. 2. Flow diagram for the crystallization system.

chemical analysis of the solution. Properties frequently chosen for indirect methods include density, viscosity, refractive index, and electrical conductivity. As discussed by Mullin (1972), these properties can often be measured with high precision, especially if the measurement is made under carefully controlled conditions in the laboratory. However, for the operation of a continuous crystallizer, the demand is usually for an in situ method, preferably one capable of continuous operation. Under these conditions, problems may arise from the temperature dependence of the property being measured. In general, density and refractive index are the least temperature sensitive properties.

The first reported use of measuring supersaturation of a solution by measuring changes in refractive index appears to be the studies by Miers (1904) and by Miers and Isaac (1906). Since that time, other researchers (Jenkens, 1925; Bunn and Emmett, 1949; Mullin et al., 1970; Mullin and Leci, 1972; Klekar, 1973) have used refractive index measurements in crystallization work.

EXPERIMENTAL

The crystallizer used in this work was a mixed-suspension, mixed-product-removal cooling crystallizer as shown in Figure 1. It was a Plexiglas cylindrical vessel equipped with three baffles and a propeller type of agitator. The overall volume was approximately 14 mm^3; however, the active volume used was 10 mm^3. A partial draft tube was achieved by the helical stainless steel cooling coil immersed in the crystallizer. Cooling was achieved by circulating ethylene glycol from a Blue M refrigeration unit. The agitator, vertically mounted in the center of the vessel, was powered by a model V-7 lightnin mixer. The direction of flow was down the center and up the outside annular space between the cooling coil and vessel wall. The agitator speed was adjustable to provide good mixing of the mother liquid and crystal suspension. The flow diagram of the apparatus is shown in Figure 2.

The feed solution was prepared and stored in an insulated 210 mm^3 stainless steel drum. An electrical immersion type of tank heater was used to heat the solution. The heater was thermostat controlled to maintain the desired temperature in the feed tank throughout the experimental runs.

The feed solution was pumped to the crystallizer by an Eastern 50W centrifugal pump that was controlled by a Variac variable powerstat. Also included in the feed line were a rotameter to monitor the flow rate, a needle valve for flow control, and a 350 nm Pall disposable filter assembly. The feed inlet to the crystallizer was from above, with discharge into the center of the vessel.

The thermostat control on the immersion heater in the feed drum produced some fluctuations in the temperature of the feed solution. A small glass heat exchanger was used in the feed line to decrease the amplitude of these fluctuations and therefore maintain better temperature control in the crystallizer.

The average outflow from the crystallizer was too small to withdraw continuously without size classification. Therefore, intermittent product withdrawal was used so that high withdrawal velocities could be achieved. To accomplish the intermittent withdrawal, a Sargent laboratory relay was used in conjunction with an adjustable time delay unit. An electrode was used to sense the liquid level. The probe was set at the maximum desired liquid level for the vessel so that when the liquid level reached the height of the probe it would complete a circuit and activate the relay-time delay system. This system would then start the withdrawal pump which ran for a preset length of time until the time delay shut off. Withdrawal times of 2, 10, or 15 s could be used. The withdrawal tubing between the crystallizer and the pump was stainless steel (9.5 mm I.D.) and wrapped with an electrical heat tape to provide some initial heating of the slurry before it was returned to the feed tank.

The differential refractometer used in the experiments was a Waters Associates model R-404. The unit has two cells, one for the reference materials and one for the sample. The refractometer measures the deflection of a light beam resulting from

the difference in refractive indices between the sample and the reference liquid. The instrument is capable of sensing changes of 1×10^{-7} RI units. The output signal from the refractometer is in millivolts. With the use of calibration curves the output could be converted to refractive index units, or in the case of the present work, to concentration units. The output was recorded by using a Beckman Instruments offner type of strip chart recorder. To insure thermal accuracy of the refractometer, a Haake FJ circulating water bath was used to keep the temperature of the refractometer constant.

The sample withdrawal port was in the side of the crystallizer as shown in Figure 1. The opening was covered with a 75 μm fine mesh screen to prevent crystals from leaving the vessel.

To provide a reference solution a saturator was installed inside the crystallizer. This was a Pyrex tube, 29 mm in diameter, and 180 mm long. The bottom of the tube was sealed using a millipore Swinnex-25 filter unit with a 2.5 mm outlet. Plastic tubing was connected to the outlet to allow liquid withdrawal. The filter unit contained 25 mm filter paper with a maximum opening of 850 nm. The top of the saturator cylinder was left open, but mounting was such that the top was above the liquid level in the crystallizer.

The saturator was filled approximately half full with potassium nitrate crystals and then filled with distilled water. The arrangement provided a supply of saturated potassium nitrate solution at the same temperature as the crystallizer and thus represented a reference for supersaturation measurements. Withdrawal from the saturator to the reference cell was periodic and was accomplished using a second Masterflex pump. If the liquid in the saturator became depleted during an experimental run, it could be momentarily lowered below the liquid level of the crystallizer and refilled with the crystal slurry. The bed of undissolved potassium nitrate crystals was more than ample to ensure a saturated solution at all times during the run.

For those experimental runs where the crystallizer temperature was greater than the room temperature, an electrical heating tape was used on all sampling lines to prevent in-line crystallization and flow blockage.

In preparing the feed solution, reagent grade potassium nitrate was used. Feed of the desired concentration was prepared by dissolving the required weight of salt in distilled water. For each series of experimental runs, the feed concentration was selected to be that of a saturated solution at a temperature 1 to 2°K above the crystallizer temperature being used. During the crystallizer operation, the feed solution was maintained at a temperature at least 3°K above the saturation temperature to ensure that all crystals were dissolved. The feed solution was pumped from the drum through a final filter, a control valve, a rotameter, and into the crystallizer.

The crystallizer was normally operated for a minimum of eight residence times to achieve steady state. Then supersaturation measurement was started. The supersaturation data were collected for two to six residence times. Sampling of the crystal suspension was then initiated. Two samples of the crystal suspension was obtained approximately ½ hr apart.

A graduated vacuum flask was employed to withdraw samples of the crystal suspension from the operating crystallizer. This method resulted in quick removal of the sample which prevented size classification and led to consistency in the method of sampling. The size of the samples varied depending upon the suspension density but were generally in the range of 400 to 800 μm^3 in size. Samples withdrawn from various locations in the crystallizer for the same run revealed similar size distributions.

The samples were immediately filtered and washed to prevent new crystallization or the dissolving of existing crystals. After the crystals were dried, they were separated and sized using a set of 76 mm, U.S. standard sieves. The crystals were then removed from each screen and weighed. From the various weights, the population density could be calculated.

RESULTS

Treatment of Data

As mentioned earlier, a sieve analysis was used to obtain the weight fractions for the various size ranges. To obtain population densities, this weight distribution

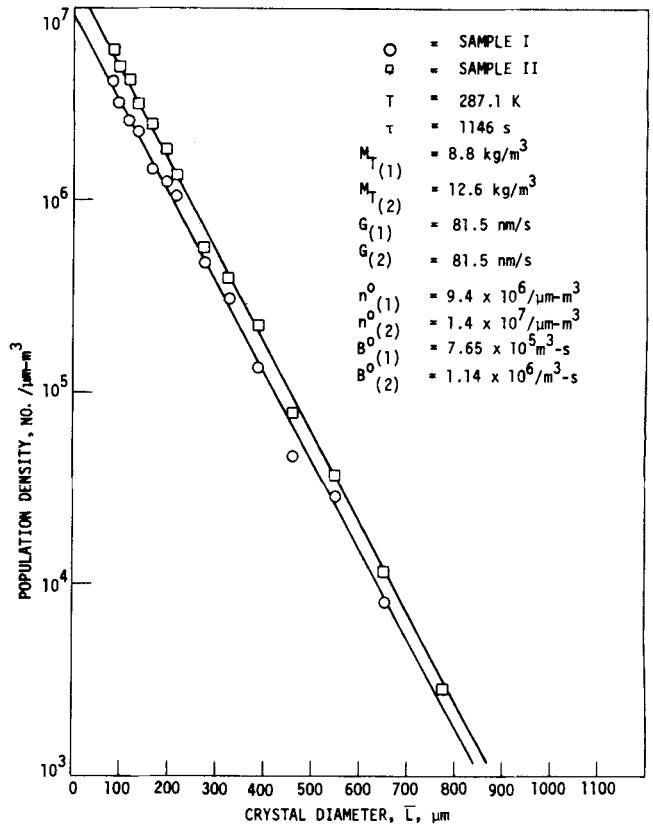

Fig. 3. Typical plot of crystal size distribution for potassium nitrate.

was converted to number of particles using

$$n = \left(\frac{W}{K_v L^3 \rho \Delta L}\right) \frac{100}{V_s} \tag{9}$$

The supersaturation measurement was made with the refractometer at a constant temperature of 308°K, selected to be well above the crystallizer temperature for all runs. The supersaturation reading was recorded over a period of two to six residence times after steady state was achieved. During this recording time, there was fluctuation in the supersaturation reading resulting from slight variations in flows and the normal cycling which occurs with an operating system. This cycling was held to ±0.5°K, but it may have been enough to be responsible for much of the fluctuation observed in supersaturation. In most cases, the fluctuation in supersaturation was on the order of ±20%. Because of this fluctuation, a time averaged value of supersaturation was obtained for each run during steady state operation.

Because the supersaturated liquid was removed for refractive index measurement through a 75 μm screen, the supersaturation measurement included the redissolved crystal of size less than 75 μm. Calculations showed that this could account for no more than 5% of the supersaturation measured.

Growth and Nucleation Rates

The fundamental relationship giving the number distribution of the crystal product obtained from a continuous MSMPR crystallizer operating at steady state is given by Equation (1). A semilog plot of this relationship gives a straight line with an intercept at $L = 0$ of n^o and a slope of $-1/G\tau$. This relationship, therefore, gives a method of determining the growth and nucleation rates from the population density data obtained for each run. A semilog plot of population density vs. size was made for each set of data as shown in Figure 3 for size distribu-

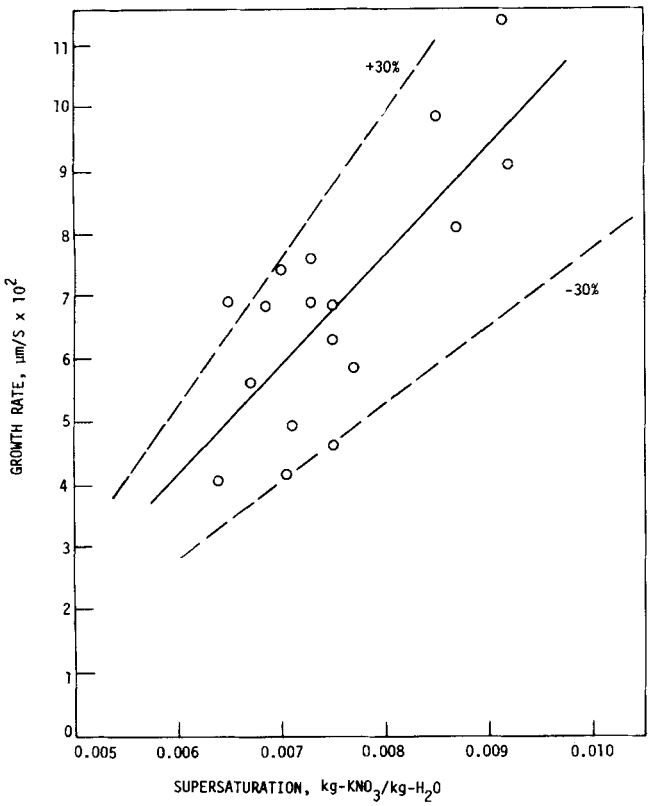

Fig. 4. Relationship between growth rate and supersaturation.

tion obtained at a crystallizer temperature of 287.1°K. An exponential least-squares analysis was completed for each plot, and the best fit intercept and slope for the data were in turn used to calculate the nucleation rate B^o and the growth rate G.

Secondary nucleation rate is a function of the suspension density in the crystallizer. For potassium nitrate, the relationship is a direct one with the suspension density M_T to the first power (Shor and Larson, 1971; Timm and Larson, 1968):

$$B^o = K_1 M_T f(s) \qquad (10)$$

In the experimental runs, the suspension density varied from one run to another. Therefore, for the calculated nucleation rates to be comparable from run to run, it was necessary to put them on a common basis. This was done by using a suspension density basis of 10Kg/m³. To achieve this, all nucleation rates were divided by the suspension density.

In order to determine the kinetic rates at various levels of supersaturation, the retention time in the crystallizer was changed. A change in retention time, while all other conditions are kept the same, results in a change in production rate for a class II system which in turn reflects a change in supersaturation. Runs were made at a wide variety of retention times varying from 13 to 50 min.

There was some scatter in the data because of the very low level of supersaturation which existed. However, the growth rates obtained showed a linear relationship with supersaturation as shown in Figure 4 for the data taken at 293°K. The data for other temperatures gave similar straight lines. The data taken at 298°K, however, exhibited excessive scatter and were difficult to interpret (Helt, 1976).

It should be noted in Figure 4 that an extrapolation of the straight line correlation of these data will not pass through the origin. Clearly, the data cover only the straight line portion of a higher-order curve. The range of supersaturation measured was relatively small, ranging between 0.0035 and 0.011 kg potassium nitrate/kg water. A higher-order relationship would therefore be needed to describe the lower portion of the growth rate curve.

Jones and Mullin (1973) observed a similar relationship in their work with potassium sulfate. They found there was a positive value of supersaturation even when the overall linear growth rate was zero. Mullin (1972) points out that this is the relationship one would expect if the Burton-Cabrera-Frank growth equation is used. This equation approximates to a growth rate proportional to the supersaturation squared at low values of supersaturation. But at high supersaturations the equation reduces to a linear relationship between growth rate and supersaturation.

TABLE 1. SUMMARY OF EXPERIMENTAL POWER LAW RELATIONSHIPS

Growth rate as function of supersaturation μm/s

283°K: $G = 11.7 - 0.003$
287°K: $G = 12.2 - 0.028$
293°K: $G = 17.8 - 0.064$
298°K: $G = 10.0 - 0.005$
$G = 29.2 - 0.147$

Nucleation rate as function of supersaturation no./m³-s

283°K: $B^o/M_T = 1.42 \times 10^{10} (s - 0.0015)^{1.79}$
287°K: $B^o/M_T = 4.79 \times 10^{9} (s - 0.002)^{1.70}$
293°K: $B^o/M_T = 1.02 \times 10^{10} (s - 0.0036)^{1.89}$
298°K: $B^o/M_T = 7.26 \times 10^{8} (s)^{1.58}$

Nucleation rate as function of growth rate no./m³-s

283°K: $B^o/M_T = (8.6 \times 10^{7}) G^{1.72}$
287°K: $B^o/M_T = (7.4 \times 10^{7}) G^{1.74}$
293°K: $B^o/M_T = (3.3 \times 10^{7}) G^{1.76}$
298°K: $B^o/M_T = (1.4 \times 10^{7}) G^{1.43}$

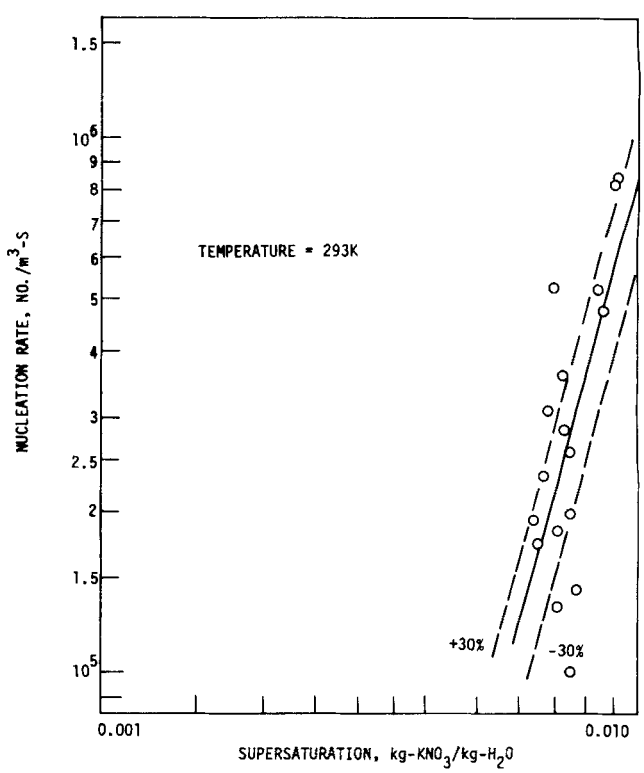

Fig. 5. Relationship between nucleation rate and supersaturation.

The correlations for the various temperatures are given in Table 1, showing the extrapolated intercept. In every case, the intercept is negative, indicating that a second-order relationship is necessary to represent the curve for the growth rate at supersaturation near zero. Note that for the 298°K data two correlations are given. The first gives the correlation for a least-square fit of the data as reported by Helt (1976). The second correlation resulted from the best straight line drawn through the data by inspection. In either case, the excessive scatter of the data leaves both points suspect, but the latter is more in line with the data taken at other temperatures.

Power law relationships were also expected for the nucleation vs. supersaturation data. As with the growth rate, a graphical approach was employed to test for the validity of Equation (7). Log-log plots of nucleation rate vs. supersaturation were made for each of the temperature levels studied. An example plot showing the 293°K data is shown in Figure 5. The best least-squares fit of the data points is shown. The slope is quite steep, resulting in a rather large unrealistic value for the power exponent m.

Secondary nucleation does not occur until some minimum supersaturation s^* is reached. It has been observed that the secondary nucleation rate is closely related to the rate at which the parent crystals are growing. At very low supersaturation, where crystal growth rate is extremely slow, contact secondary nucleation would normally not occur. The level of supersaturation which is ineffective to produce secondary nucleation should, therefore, correspond to the second-order portion of the growth curve. Consequently, an s^* was calculated from the linear growth rate correlation and used in a Miers nucleatic model of the form

$$B^o = K_1' M_T^j (s - s^*)^m \qquad (11)$$

The fit of the 293°K nucleation data to this model is shown in Figure 6, and the correlations for the other

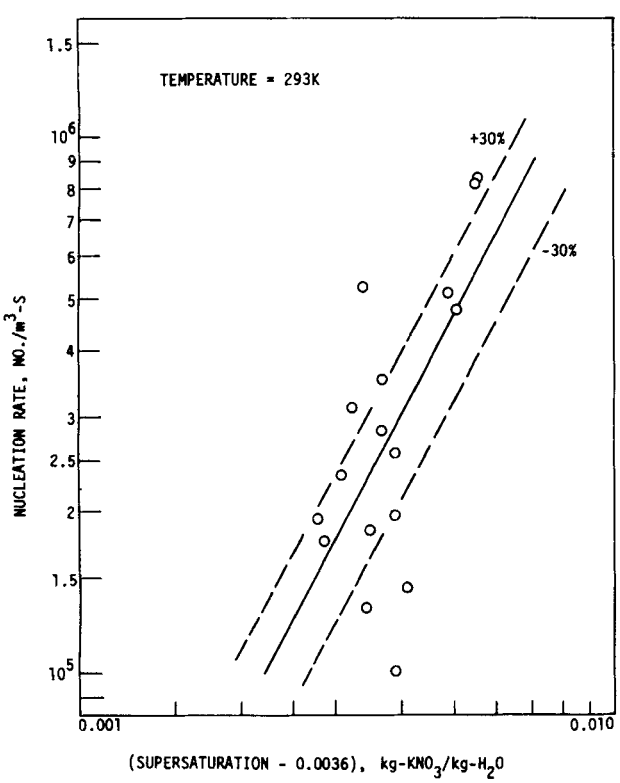

Fig. 6. Relationship between nucleation rate and $(s - s^*)$.

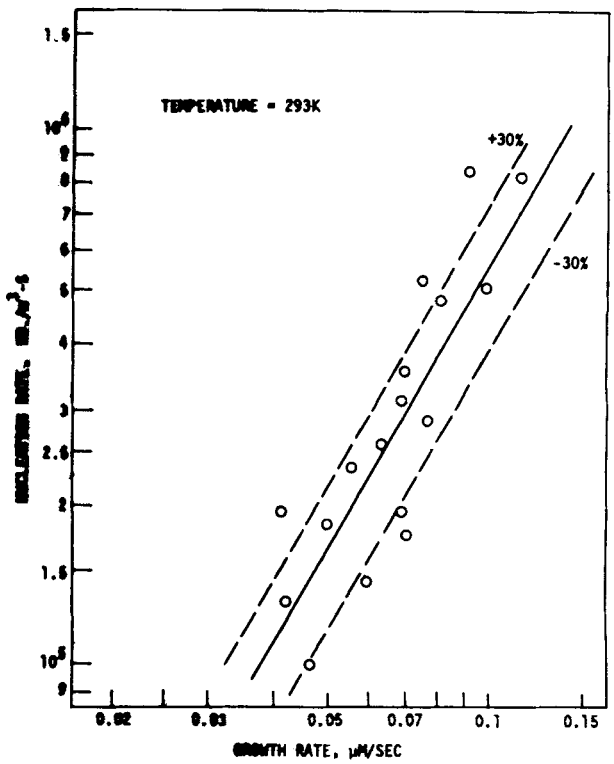

Fig. 7. Relationship between nucleation rate and growth rate.

temperatures are shown in Table 1. These agree very well with the work of Genck (1969). Note, however, that the data for 298°K are somewhat in variance with the other temperatures, reflecting the excessive scatter of those experiments.

In developing the power law expressions, it was shown that supersaturation could be eliminated from the expression to obtain Equation (8). By combining Equations (2) and (8), the following relationship is obtained:

$$B^o = K_N' M_T^j G^i \qquad (12)$$

A log-log plot of nucleation rate vs. growth rate should be linear with a slope of i. Such plots were prepared for all of the temperatures studied. The plot for the 293°K data is shown in Figure 7, and the correlations for the other temperatures are shown in Table 1. The slopes yield a value for i of 1.7. As was shown earlier, the growth rate is an approximately linear function of supersaturation. It was also shown during the section on model development that $i = (m/n)$. We have seen that n is approximately equal to 1.0 and that i is approximately equal to 1.7; therefore, m should be equal to 1.7, as was found in using the relationship of Equation (11).

It should also be noted that the data show much less scatter than the plots involving supersaturation. Since this plot doesn't involve data from the supersaturation measurement, it indicates that the scatter in earlier plots can be attributed to errors in measurement of the supersaturation. This is expected, since the supersaturation value is very small and quite sensitive to small changes in temperature, pressure, and impurities.

Temperature Dependency

The activation energies for growth and nucleation were determined from the correlations given in Table 1, assuming that only the rate constants K_1' and K_2 to be temperature dependent and that they followed an Arrhenius type of temperature dependency.

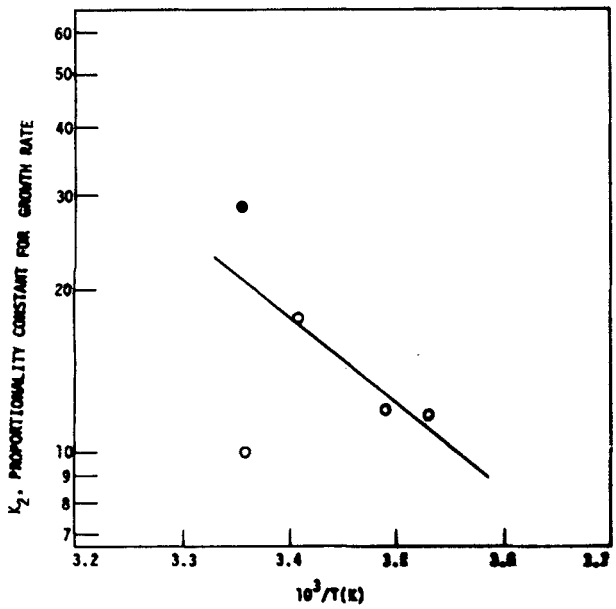

Fig. 8. Temperature dependency of proportionality constant for growth rate.

TABLE 2. COMPLETE KINETIC RELATIONSHIPS

Activation energy for growth = 31 *MJ*/kg mole

$$G = 4.8 \times 10^6 \exp(-31/RT)\,(s)^{1.0}$$

Activation energy for nucleation = −108 *MJ*/kg mole

$$B^o/M_T = 3.0 \times 10^{-10} \exp(108/RT)\,(s - s^*)^{1.7}$$

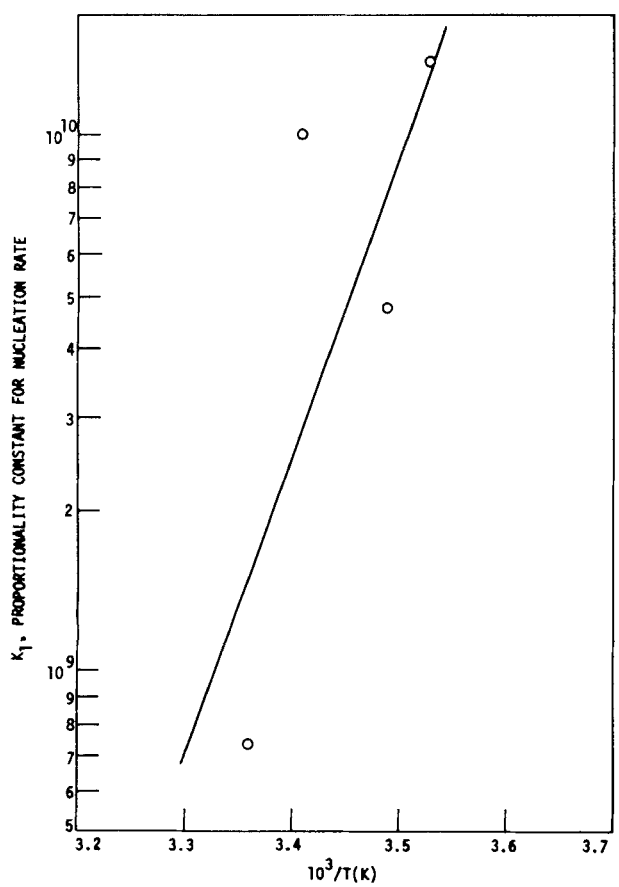

Fig. 9. Temperature dependency of proportionality constant for nucleation rate.

The rate constants for growth are plotted as a function of temperature in Figure 8, and the resulting correlation is given in Table 2. Included on the plot are two points for the results at 298°K, reflecting the two correlations reported in Table 1. The activation energy obtained is 31 *MJ*/kg mole. This compares favorably with 32 *MJ*/kg mole calculated from Genck's (1969) data.

The nucleation rate constants are plotted in Figure 9, and the correlation is shown in Table 2. Here the slope is positive, indicating that Arrhenius types of kinetic models do not explain nucleation temperature dependency. The data show that nucleation rate decreases as temperature increases. This was also observed qualitatively by Genck (1969) for potassium nitrate and by Sikdar and Randolph (1976) for potassium sulfate and magnesium sulfate.

The temperature dependency of the growth rate can also be investigated by observing the growth rate change for a given residence time when the temperature increases. By using residence time in place of supersaturation as a constant parameter, the supersaturation measurement errors are avoided. The resulting comparisons are shown in Table 3. It is seen from this table that for a constant residence time the growth rate increases as the temperature increases. It can also be seen that as residence time increases, the growth rate decreases.

DISCUSSION

The most interesting result of this work is that for a given supersaturation, the nucleation rate is inversely

TABLE 3. GROWTH RATE AS A FUNCTION OF TEMPERATURE AND RESIDENCE TIME

	Growth rates, μm/s			
τ, s	283°K	287°K	293°K	298°K
<900			0.115	0.116
			0.126	
900 to 1 200	0.074	0.077	0.092	0.090
	0.078	0.079	0.095	0.092
	0.078	0.084	0.099	0.096
		0.086	0.100	0.107
		0.089	0.107	
		0.089		
1 200 to 1 500	0.053	0.062	0.075	0.079
	0.064	0.064	0.082	0.085
	0.068	0.070	0.088	0.089
	0.069	0.071		0.089
		0.072		
		0.073		
		0.077		
1 500 to 1 800		0.055	0.063	0.055
		0.056	0.069	0.068
		0.058	0.069	0.070
		0.059	0.070	
			0.070	
			0.077	
1 800 to 2 100	0.045	0.039	0.056	0.054
	0.048	0.050	0.059	0.058
2 100 to 2 400	0.040	0.044	0.050	0.057
		0.047		
>2 400	0.037	0.038	0.041	0.040
		0.040	0.042	0.046
		0.042	0.046	

related to temperature. This is opposite of what would normally be found with Arrhenius type of kinetics. It is not the first time, however, that such a relation has been observed. Kern and Abegg (1973) reported such a change with a proprietary substance, and Genck (1969) previously observed this with potassium nitrate. In both of these earlier cases, supersaturation was not measured. Sikdar and Randolph (1976) reported similar results for K_2SO_4 and $MgSO_4 \cdot 7H_2O$. Genck (1969) suggested that the decrease in nucleation rate with increasing temperature was the result of a decrease in the supersaturation level; however, the measurement of supersaturation in the present work does not support that conclusion.

To explain this phenomenon, one must postulate a mechanism that might be occurring at the crystal surface. Surface diffusion and overall activation energy could both play a major role in causing the observed relationship. In either case, one must start by looking at the surface characteristics of a growing crystal. The concept put forth by Powers (1963) is the most plausible explanation. He presumed that the surface of the crystal is covered by a fluidized layer and that this layer is made up of molecules of solute loosely bound to the growing crystal face.

For growth to occur, the molecules are drawn from this fluidized layer to be anchored in the true lattice bondings on the growing layer fronts. This involves surface diffusion of the molecular aggregates. If, as would be expected, the surface diffusion rate and the surface integration rate increase with temperature, then the incorporation of the molecules into the lattice would occur more quickly as a result of temperature increase. This means that at higher temperatures there would be fewer molecules available in the fluidized layer, and it would not be as extensive as it was at lower temperatures.

Powers (1963) also proposed that secondary nucleation is very dependent upon the fluidized layer. He postulated that secondary nucleation occurs when fluid shear and collisions cause some of the fluidized layer to be drawn off to form new nuclei. If at a higher temperature the increased surface diffusion rate and increased reaction rate deplete the fluidized layer faster than it is regenerated by fresh solute from the solution, there would be less secondary nucleation. This explains the decrease in nucleation rate as temperature is increased.

Powers (1963), Melia and Moffitt (1964), and Sung et al. (1973) all point out that many times secondary nucleation is associated with dendritic types of growths appearing on the surface of the parent crystal. The shearing action of the fluid and collisions within the system break off the dendrites to form new nuclei. It is worthwhile to consider how increased surface diffusion, resulting from increased temperature, might influence the growth of dendrites. If dendritic growth is an important part of secondary nucleation, then the fewer the number of dendrites, the lower the nucleation rate.

In a study of ice crystals, Fletcher (1958) points out that surface diffusion provides a stabilizing mechanism by tending to destroy any perturbations on the growth surface. He states that the effect of surface diffusion is very considerable and has a large influence on the growth morphology. Van Hook (1961) discusses a correlation between d, the diameter of the crystal, and x_t, the thickness of the crystal medium interface. If $x_t << d$, polyhedra forms prevail, but if $x_t >> d$, then dendrites appear. Thus, if surface diffusion is increased owing to increased temperatures, it is likely that dendritic growth and the secondary nucleation rate will be decreased.

The second major influence of the temperature on the observed nucleation rate can come from the overall activation energy considerations. Decreased nucleation rates with increasing temperature have been observed in melts. If the crystal surface is indeed covered with a fluidized layer of solute as Powers (1963) suggests, then the nucleation behavior might be considered to be much the same as nucleation from a melt. That is, nuclei are formed in the layer to be subsequently dislodged as a result of collision. Some insight might then be gained by looking at the mechanism which causes inverse nucleation rate in melts.

Following the development of Mullin (1972), it can be shown how the abnormal nucleation characteristic observed in melts occurs. First, the nucleation rate is expressed in the form of the Arrhenius reaction velocity equation commonly used for the rate of thermally activated process:

$$B^o = A_1 \exp(-\Delta G/k_bT) \tag{13}$$

The Gibbs-Thomson relationship can be written as

$$\ln S = \frac{2\sigma v}{k_bTr} \tag{14}$$

This then gives

$$-\Delta G_v = \frac{2\sigma}{r} = \frac{k_bT \ln (S)}{v} \tag{15}$$

It can be shown that

$$\Delta G_{crit} = \frac{16\pi\sigma^3v^2}{3[k_bT \ln (S)]^2} \tag{16}$$

and from Equation (13)

$$B^o = A_1 \exp\left[\frac{-16\pi\sigma^3v^2}{3k_b^3T^3(\ln S)^2}\right] \tag{17}$$

This equation indicates that three main variables govern the rate of nucleation: temperature T, supersaturation S, and interfacial tension σ.

Tamman (1925) observed that in dealing with melts, the rate of nucleation usually increases exponentially as supersaturation increases. But as higher levels of supersaturation are reached, the nucleation rate reaches a maximum and subsequently decreases. Tamman suggested that this behavior was caused by the sharp increase in viscosity with supercooling which restricted molecular movement and inhibited the formation of ordered crystal structures. Turnbull and Fisher (1949) quantified this observed behavior with a modified form of Equation (17)

$$B^o = A_1' \exp\left[\frac{-16\pi\sigma^3v^2}{3k_b^3T^3(\ln S)^2} + \frac{\Delta G'}{k_bT}\right] \tag{18}$$

which includes a viscosity term. When $\Delta G'$, the activation energy for molecular motion across the embryo matrix interface, is exceptionally large (as in the case of highly viscous liquids and glasses), the other exponential term is small, because under these conditions S is generally large. $\Delta G'$ then becomes the dominant factor in the rate equation, and a decrease in nucleation rate is predicted.

Previously reported experimental observations of this reversal of the nucleation rate have been confined to melts, but they should also be expected in highly viscous solutions. Mullin and Leci (1969) also observed such a behavior in aqueous solutions of citric acid.

Since the apparent reversal of nucleation rate was observed in the present study using potassium nitrate, it could be concluded that the activation energy $\Delta G'$ of this system must be quite large. This would result in the second exponential term of Equation (18) being

dominant. In the temperature range studied, the viscosity term would then have the controlling influence over the observed nucleation rate.

Finally, it is observed that the metastable region of supersaturation, the region of supersaturation where secondary nucleation does not occur, appears to coincide with a higher-order portion of the growth vs. supersaturation curve. This observation supports the importance of the growth mechanism on the rate of secondary nucleation. In the low supersaturation region, where growth follows a second order or higher relationship with supersaturation, the observed growth rates are very, very low, and there is no apparent nucleation.

ACKNOWLEDGMENT

The authors acknowledge the financial support provided by National Science Foundation through Grant 73-03864, to the E. I. du Pont de Nemours Co., Phillips Petroleum Co., and Union Carbide. They also acknowledge the support of the Iowa State University Engineering Research Institute.

NOTATION

A_1 = proportionality constant
A_1' = proportionality constant
B^o = nucleation rate
c = solute concentration in supersaturated solution
c_s = saturation concentration of solute
d = equivalent diameter of crystal
G = growth rate of crystals
ΔG = overall excess free energy
$\Delta G'$ = activation energy for molecular motion across the embryo matrix interface
ΔG_{crit} = overall excess free energy of a particle with radius r_c
ΔG_v = free energy change per unit volume
i = m/n, nucleation rate power dependency on growth rate
j = nucleation order related to M_T
k_b = Boltzmann constant
K_N = proportionality constant for nucleation rate as function of growth rate
K_N' = proportionality constant for nucleation rate temperature effects as function of growth rate.
K_v = volumetric shape factor
K_1 = proportionality constant for nucleation rate as function of supersaturation
K_1' = proportionality constant for nucleation rate temperature effects as function of supersaturation
K_2 = proportionality constant for growth rate as function of supersaturation
L = crystal size, equivalent diameter
$\overline{L}$ = arithmetic average crystal diameter
ΔL = width of size fraction, $L_2 - L_1$
m = nucleation rate power dependency on supersaturation
M_T = suspension density
n = population density of crystal suspension
n = (as exponent) growth rate power dependency on supersaturation
n^o = population density of zero size particles or nuclei
r = particle radius
s = $c - c_s$, supersaturation
s^* = constant value of supersaturation used for correction of power law expressions
S = supersaturation ratio, c/c_s
T = temperature
v = molecular volume
V_s = volume of sample
W = weight of crystals
x_t = thickness of crystal medium interface
ρ = density of crystals
τ = V/Q, residence time
σ = surface energy

LITERATURE CITED

Bunn, C. W., and H. Emmett, "Crystal Growth From Solution," *Disc. Faraday Soc.*, **5**, 119-144 (1949).

Fletcher, N. H., "Size Effect in Heterogeneous Nucleation," *J. Chem. Phys.*, **29**, 572-576 (1958).

Genck, W. J., "Temperature Effects on Growth and Nucleation Rates in Mixed Suspension Crystallization," PhD thesis, Iowa State Univ., Ames (1969).

Helt, James E., "Effects of Supersaturation and Temperature on Nucleation and Crystal Growth in a MSMPR Crystallizer," unpublished PhD thesis, Iowa State Univ., Ames (1976).

Jenkins, J. D., "The Effects of Various Factors Upon the Velocity of Crystallization on Substances from Solution," *Am. Chem. Soc., J.*, **47**, 903-922 (1925).

Jones A. G., and J. W. Mullin, "Crystallization Kinetics of Potassium Sulfate in a Draft-Tube Agitated Vessels," *Trans. Inst. Chem. Engrs.*, **51**, 302-308 (1973).

Kern, W. G., and C. F. Abegg, "An Industrial Experience with the Population Balance Approach to Crystallization," paper presented at AIChE meeting, New Orleans, La. (1973).

Klekar, S. A., "*In situ* Measurement of Supersaturation in Crystallization from Solution," MS thesis, Iowa State Univ., Ames (1973).

Melia, T. P., and W. P. Moffitt, "Secondary Nucleation From Aqueous Solutions," *Ind. Eng. Chem. Fundamentals*, **3**, No. 4, 313-317 (1964).

Miers, H. A., "An Enquiry Into the Variation of Angles Observed in Crystals: Especially of Potassium-Alum and Ammonium-Alum," *Phil. Trans. Royal Soc.*, **A202**, 459-524 (1904).

———, and F. J. Isaac, "The Refractive Indices of Crystallizing Solutions," *J. Chem. Soc. Trans.*, **89**, 413-454 (1906).

Mullin, J. W., *Crystallization*, Butterworths, London, England (1972).

———, and C. L. Leci, "Some Nucleation Characteristics of Aqueous Citric Acid Solutions," *J. Crystal Growth*, **5**, 75 (1969).

———, "Desupersaturation of Seeded Citric Acid Solutions in a Stirred Vessel," *AIChE Symposium Ser. No. 121*, **68**, 8-20 (1972).

Mullin, J. W., M. Chakraborty, and K. Mehta, "Nucleation and Growth of Ammonium Sulfate Crystals From Aqueous Solution," *J. Appl. Chem.*, **20**, 367-371 (1970).

Nielsen, A. E., *Kinetics of Precipitation*, MacMillan, N.Y. (1964).

Powers, H. E. C., "Nucleation and Early Crystal Growth," *J. Ind. Chemist*, 351-355 (1963).

Randolph, A. D., and M. A. Larson, *Theory of Particulate Processes*, Academic Press, N.Y. (1971).

Sikdar, S. K., and A. D. Randolph, "Secondary Nucleation of Two Fast Growth Systems in a Mixed Suspension Crystallizer: Magnesium Sulfate and Critic Acid Water Systems," *AIChE J.*, **22**, No. 1, 110 (1976).

Shore, S. M., and M. A. Larson, "Effects of Additives on Crystallization Kinetics," *Chem. Eng. Progr. Symposium Ser. No. 110*, **67**, 32-42 (1971).

Sung, C. Y., J. Eastrin, and G. R. Youngquist, "Secondary Nucleation of Magnesium Sulfate by Fluid Shear," *AIChE J.*, **19**, 957-962 (1973).

Tamman, G., *States of Aggregation*, R. F. Mehl, trans., van Nostrand, N.Y. (1925).

Timm, D. C., and M. A. Larson, "Effect of Nucleation Kinetics on the Dynamic Behavior of a Continuous Crystallizer," *AIChE J.*, **14**, No. 3, 452 (1968).

Turnbull, D., and J. C. Fisher, "Rate of Nucleation in Condensed Systems," *J. Chem. Phys.*, **17**, 71 (1949).

Van Hook, A., *Crystallization: Theory and Practice*, Reinhold, N.Y. (1961).

Manuscript received September 7, 1976; revision received July 18, and accepted August 10, 1977.